PHYSICAL REVIEW B **92**, 180505(R) (2015)

Nodal superconductivity and superconducting dome in the layered superconductor $Ta_4Pd_3Te_{16}$

J. Pan,[1] W. H. Jiao,[2,*] X. C. Hong,[1] Z. Zhang,[1] L. P. He,[1] P. L. Cai,[1] J. Zhang,[1] G. H. Cao,[2,3] and S. Y. Li[1,4,†]
[1]*State Key Laboratory of Surface Physics, Department of Physics, and Laboratory of Advanced Materials, Fudan University, Shanghai 200433, China*
[2]*Department of Physics, Zhejiang University, Hangzhou 310027, China*
[3]*Collaborative Innovation Center of Advanced Microstructures, Nanjing 210093, China*
[4]*Collaborative Innovation Center of Advanced Microstructures, Fudan University, Shanghai 200433, China*
(Received 16 September 2014; revised manuscript received 9 September 2015; published 9 November 2015)

We measured the low-temperature thermal conductivity of a layered superconductor with quasi-one-dimensional characteristics, the ternary telluride $Ta_4Pd_3Te_{16}$ with a transition temperature $T_c \approx 4.3$ K. The significant residual linear term of thermal conductivity in zero magnetic field and its rapid field dependence provide evidence for nodes in the superconducting gap. By measuring resistivity under pressure, we reveal a superconducting dome in the temperature-pressure phase diagram. The existence of gap nodes and a superconducting dome suggest unconventional superconductivity in $Ta_4Pd_3Te_{16}$, which may relate to a charge-density-wave instability in this low-dimensional compound.

DOI: 10.1103/PhysRevB.92.180505 PACS number(s): 74.25.fc, 74.20.Rp, 74.62.Fj, 74.70.Dd

Finding unconventional superconductors and understanding their superconducting mechanism are some of the main themes in condensed matter physics [1]. The term "unconventional" first means the superconducting pairing mechanism is not phonon mediated. This usually manifests as a superconducting dome neighboring a magnetic order in the phase diagram, and spin fluctuations are considered as the major pairing glue [1]. Second, the term "unconventional" means the wave function of Cooper pairs is not *s* wave. Symmetry-imposed nodes (gap zeros) are often observed, such as in *d*-wave cuprate superconductors and the heavy-fermion superconductor $CeCoIn_5$ [2,3], and in the *p*-wave superconductor Sr_2RuO_4 [4]. Note that iron-based superconductors are exceptions, likely with the form of $s_\pm$ wave [5]. The superconducting gap symmetry and structure provide important clues to the underlying pairing mechanism.

Unconventional superconductivity usually resides in quasi-two-dimensional (Q2D) compounds, such as cuprate and iron-based superconductors, $CeCoIn_5$, Sr_2RuO_4, and organic superconductors κ-bis(ethylenedithio)tetrathiafulvalene salts [κ-(BEDT-TTF)$_2X$] [1]. When further reducing the dimensionality, namely, in quasi-one-dimensional (Q1D) superconductors represented by the organic compounds tetramethyltetraselenafulvalenium salts [(TMTSF)$_2X$] ($X = PF_6$, ClO_4) [6,7], the pairing symmetry and mechanism are also likely unconventional [8]. In this sense, low dimensionality is important for the appearance of unconventional superconductivity [9].

Recently, the ternary telluride $Ta_4Pd_3Te_{16}$ [10] was found to be a layered superconductor with Q1D characteristics [11]. The T_c is about 4.5 K at ambient pressure. It has relatively flat Ta-Pd-Te layers in the $(\bar{1}03)$ plane, which contains $PdTe_2$, $TaTe_3$, and Ta_2Te_4 chains along the crystallographic *b* axis, as illustrated in Fig. 1. It will be very interesting to check whether unconventional superconductivity exists in this low-dimensional compound.

In this Rapid Communication, we present the low-temperature thermal conductivity measurements of a $Ta_4Pd_3Te_{16}$ single crystal down to 80 mK, which clearly demonstrates that there are nodes in the superconducting gap. Furthermore, a superconducting dome in the temperature-pressure phase diagram is revealed by resistivity measurements under pressures up to 21.9 kbar. These results suggest unconventional superconductivity in $Ta_4Pd_3Te_{16}$. We discuss the possible origin of this superconducting state.

Single crystals of $Ta_4Pd_3Te_{16}$ were grown by a self-flux method [11]. The shiny crystals, which are in a flattened needle shape, have the longest dimension along the *b* axis (the chain direction). The largest natural surface with typical dimensions of 2.5×0.25 mm^2 is in the $(\bar{1}03)$ plane, which is the $a'b$ plane in Fig. 1(a). The thickness along the c^* direction is about 0.1 mm. The dc magnetization measurements were performed in a superconducting quantum interference device (SQUID) [magnetic properties measurement system (MPMS), Quantum Design], with an applied field of $H = 10$ Oe parallel to the *b* direction. Four contacts were made directly on the sample surfaces with silver paint, which were used for both resistivity and thermal conductivity measurements along the *b* direction at ambient pressure. The resistivity was measured in a ^{4}He cryostat from 300 to 2 K, and in a ^{3}He cryostat down to 0.3 K. The thermal conductivity was measured in a dilution refrigerator, using a standard four-wire steady-state method with two RuO_2 chip thermometers, calibrated *in situ* against a reference RuO_2 thermometer. For resistivity measurements under pressure, the contacts were made with silver epoxy. Samples were pressurized in a piston-cylinder clamp cell made of Be-Cu alloy, with Daphne oil as the pressure media. The pressure inside the cell was determined from the T_c of a tin wire.

Figure 2(a) shows the typical low-temperature dc magnetization of the $Ta_4Pd_3Te_{16}$ single crystal. With the zero-field-cooling process, a sharp diamagnetic superconducting transition is observed at $T_c \approx 4.3$ K. In Fig. 2(b), the resistivity of the $Ta_4Pd_3Te_{16}$ single crystal (sample S1) in zero field is plotted. The resistivity decreases smoothly from room temperature to T_c. Fitting the data between 7 and 25 K to $\rho(T) = \rho_0 + AT^n$

*Present address: Department of Physics, Zhejiang University of Science and Technology, Hangzhou 310023, China.
†shiyan_li@fudan.edu.cn

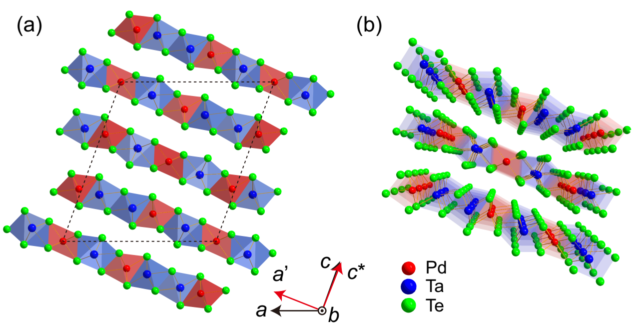

FIG. 1. (Color online) Crystal structure of $Ta_4Pd_3Te_{16}$. (a) A view parallel to the *ac* plane. The compound crystallizes in space group $I2/m$ with a monoclinic unit cell of $a = 17.687(4)$ Å, $b = 3.735(1)$ Å, $c = 19.510(4)$ Å, and $\beta = 110.42°$. The crystal structure has relatively flat Ta-Pd-Te layers in the $(\bar{1}03)$ plane, which is the largest natural surface of as-grown single crystals. For convenience, we define the a' direction as [301], so that the $(\bar{1}03)$ plane is the $a'b$ plane. c^* is the direction perpendicular to the $a'b$ plane. The Pd atoms are octahedrally coordinated, forming edge-sharing $PdTe_2$ chains along the b axis. (b) A three-dimensional perspective view along the b axis. The $PdTe_2$ chains are separated by $TaTe_3$ chains and Ta_2Te_4 double chains.

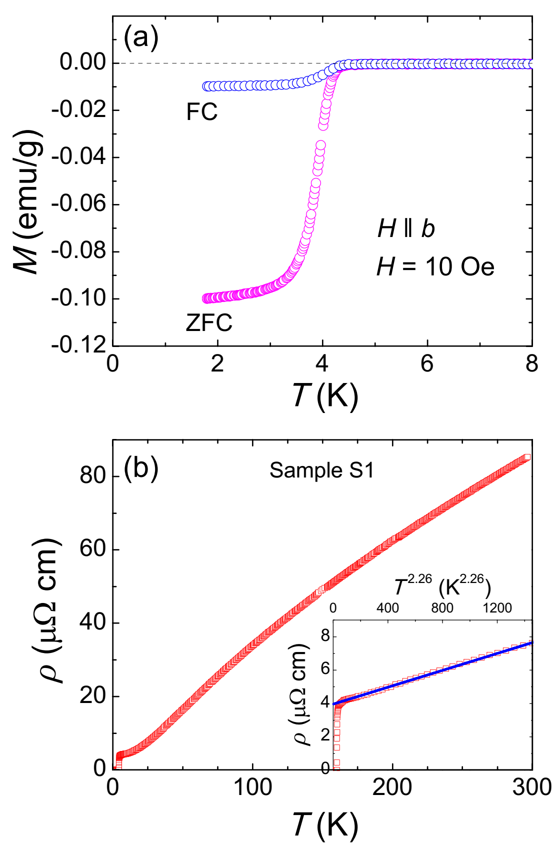

FIG. 2. (Color online) (a) The dc magnetization at $H = 10$ Oe for a $Ta_4Pd_3Te_{16}$ single crystal, with both zero-field-cooling (ZFC) and field-cooling (FC) processes. (b) The resistivity $\rho(T)$ along the b direction of the $Ta_4Pd_3Te_{16}$ single crystal (sample S1) in zero field. The data between 7 and 25 K can be well fitted to $\rho(T) = \rho_0 + AT^n$, giving a residual resistivity $\rho_0 = 3.96$ $\mu\Omega$ cm and $n = 2.26$, as shown in the inset.

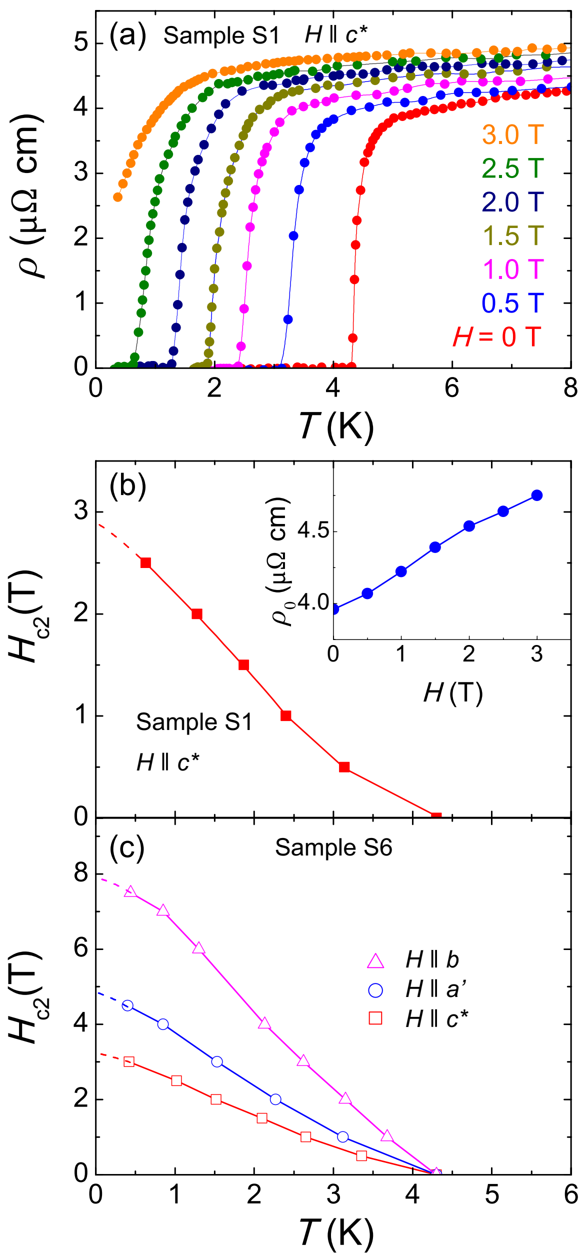

FIG. 3. (Color online) (a) Low-temperature resistivity of the $Ta_4Pd_3Te_{16}$ single crystal (sample S1) in a magnetic field $H \parallel c^*$ up to 3 T. (b) The upper critical field H_{c2} of sample S1, defined by $\rho = 0$. The dashed line is a guide to the eye, which points to $H_{c2}(0) \approx 2.9$ T. The inset shows the field dependence of ρ_0. (c) The H_{c2} of the $Ta_4Pd_3Te_{16}$ single crystal (sample S6) for $H \parallel b$, a', and c^*. The extrapolated H_{c2} values at zero temperature are 7.9, 4.8, and 3.2 T, respectively.

gives a residual resistivity $\rho_0 = 3.96$ $\mu\Omega$ cm and $n = 2.26$. The $T_c = 4.3$ K is defined by $\rho = 0$, which agrees well with the magnetization measurement.

To determine the upper critical field $H_{c2}(0)$ of $Ta_4Pd_3Te_{16}$, we measure the resistivity of sample S1 down to 0.3 K in various magnetic fields along the c^* direction. Figure 3(a) shows the low-temperature resistivity in fields up to 3 T. The temperature dependence of H_{c2}, defined by $\rho = 0$ on the resistivity curves in Fig. 3(a), is plotted in Fig. 3(b). The dashed line is a guide to the eye, which points to $H_{c2}(0) \approx 2.9$ T. The inset shows the field dependence of ρ_0, which manifests positive magnetoresistance, with $\rho_0(2\ \mathrm{T}) = 4.54\ \mu\Omega$ cm.

The anisotropy of H_{c2} along the b, a', and c^* directions for sample S6 is shown in Fig. 3(c). The resistivity data of sample S6 are not shown, and the H_{c2} is also defined by $\rho = 0$. Along three directions, $H_{c2}(0) \approx 7.9$, 4.8, and 3.2 T are estimated from Fig. 3(c). The initial H_{c2} slopes are -1.61, -0.85, and -0.53 T/K, which corresponds to the H_{c2} ratio of 3.0 : 1.6 : 1 near T_c for $H \parallel b : a' : c^*$. According to the anisotropic Ginzburg-Landau (GL) theory $H^i_{c2}/H^j_{c2} = \sqrt{\rho_j}/\sqrt{\rho_i}$ [12], the resistivity ratio $\rho_{c^*} : \rho_{a'} : \rho_b \approx 9.0 : 3.5 : 1$ is roughly estimated. This anisotropy is consistent with the calculated anisotropic electronic band structure of layered $Ta_4Pd_3Te_{16}$ with Q1D characteristics [13]. Note that this ratio is much smaller than those of quasi-1D superconductors $LiMo_6O_{17}$ and $(TMTSF)_2PF_6$ [12,14,15].

Low-temperature heat transport is an established bulk technique to probe the superconducting gap structure [16]. The thermal conductivity results of the $Ta_4Pd_3Te_{16}$ single crystal (sample S1) are presented in Fig. 4. Figure 4(a) shows the temperature dependence of thermal conductivity in a magnetic field $H \parallel c^*$ up to 2 T, plotted as κ/T vs T. The thermal conductivity at very low temperature can be usually fitted to $\kappa/T = a + bT^{\alpha-1}$ [17,18], in which the two terms aT and bT^{α} represent contributions from electrons and phonons, respectively. The power α is typically between 2 and 3, due to specular reflections of phonons at the boundary [17,18]. Since all the curves in Fig. 4(a) are roughly linear, we fix α to 2. The low values of α have been previously observed in several superconductors, for example, $Cu_{0.06}TiSe_2$ ($\alpha \approx 2.27$) and KFe_2As_2 ($\alpha \approx 2$) [19,20]. Here, we only focus on the electronic term.

In zero field, the fitting gives a residual linear term with the coefficient $\kappa_0/T \equiv a = 1.96 \pm 0.02$ mW K^{-2} cm^{-1}. This value is more than 30% of the normal-state Wiedemann-Franz law expectation $\kappa_{N0}/T = L_0/\rho_0(0\ \mathrm{T}) = 6.19$ mW K^{-2} cm^{-1}, where $L_0 = 2.45 \times 10^{-8}$ W Ω K^{-2} is the Lorenz number and $\rho_0(0\ \mathrm{T}) = 3.96\ \mu\Omega$ cm. In nodeless superconductors, all electrons become Cooper pairs as $T \to 0$ and there are no fermionic quasiparticles to conduct heat. Therefore, there is no residual linear term of κ, i.e., $\kappa_0/T = 0$. However, for unconventional superconductors with nodes in the superconducting gap, the nodal quasiparticles will contribute a finite κ_0/T in zero field [16]. For example, $\kappa_0/T = 1.41$ mW K^{-2} cm^{-1} for the overdoped d-wave cuprate superconductor $Tl_2Ba_2CuO_{6+\delta}$ (Tl-2201), which is about 36% of its κ_{N0}/T [21], and $\kappa_0/T = 17$ mW K^{-2} cm^{-1} for the p-wave superconductor Sr_2RuO_4, which is about 9% of its κ_{N0}/T [22]. The significant κ_0/T (>30% κ_{N0}/T) of $Ta_4Pd_3Te_{16}$ in zero field rules out the case that it results from a small nonsuperconducting metallic portion in the sample, thus it is strong evidence for the presence of nodes in the superconducting gap [16].

From Fig. 4(a), a small field $H = 0.2$ T has significantly increased the κ/T. Above $H = 1$ T, κ/T tends to saturate. For $H = 1.5$ and 2 T, $\kappa_0/T = 5.07 \pm 0.05$ and 5.16 ± 0.04 mW K^{-2} cm^{-1} were obtained from the fittings, respectively. The value of κ_0/T for $H = 2$ T roughly meets the normal-state Wiedemann-Franz law expectation $L_0/\rho_0(2\ \mathrm{T}) = 5.40$ mW K^{-2} cm^{-1}, which validates our

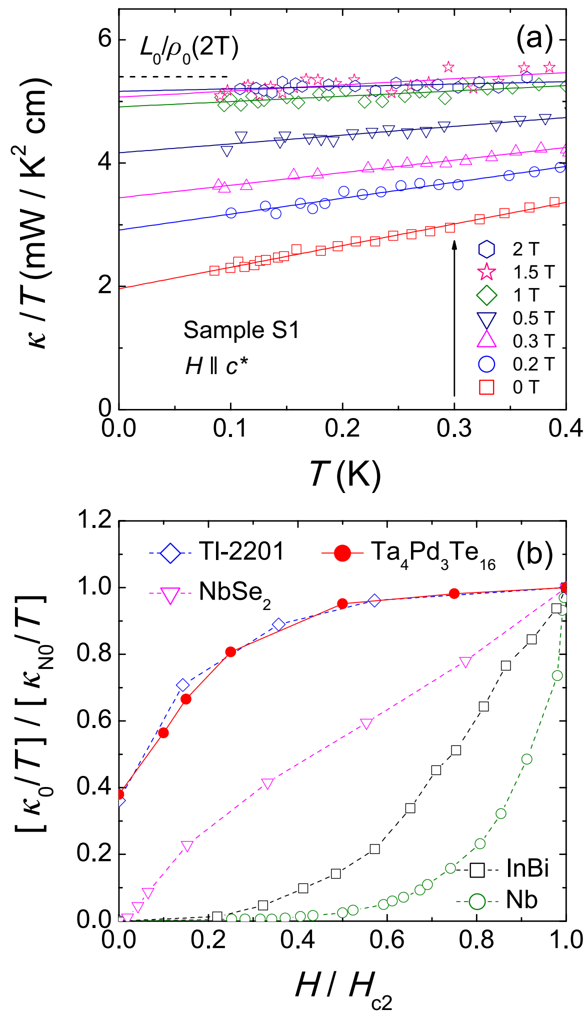

FIG. 4. (Color online) (a) Low-temperature thermal conductivity of $Ta_4Pd_3Te_{16}$ (sample S1) in magnetic fields up to 2 T, applied along the c^* direction. All the curves are roughly linear. The solid lines are fits to $\kappa/T = a + bT$. The dashed line is the normal-state Wiedemann-Franz law expectation $L_0/\rho_0(2\ \mathrm{T})$, where L_0 is the Lorenz number 2.45×10^{-8} W Ω K^{-2} and $\rho_0(2\ \mathrm{T}) = 4.54\ \mu\Omega$ cm. (b) Normalized κ_0/T of $Ta_4Pd_3Te_{16}$ as a function of H/H_{c2}. Similar data of the clean s-wave superconductor Nb [23], the dirty s-wave superconducting alloy InBi [24], the multiband s-wave superconductor $NbSe_2$ [25], and an overdoped d-wave superconductor Tl-2201 [21] are also shown for comparison. The normalized $\kappa_0(H)/T$ of $Ta_4Pd_3Te_{16}$ clearly mimics that of Tl-2201.

method of extrapolating to $T \to 0$. We take $H = 2$ T as the bulk $H_{c2}(0)$ of $Ta_4Pd_3Te_{16}$. To choose a slightly different bulk $H_{c2}(0)$ does not affect our discussions of the field dependence of κ_0/T below.

In Fig. 4(b), the normalized κ_0/T of $Ta_4Pd_3Te_{16}$ is plotted as a function of H/H_{c2}, together with the clean s-wave superconductor Nb [23], the dirty s-wave superconducting alloy InBi [24], the multiband s-wave superconductor $NbSe_2$ [25], and the overdoped d-wave cuprate superconductor Tl-2201 [21]. For $Ta_4Pd_3Te_{16}$, the field dependence of κ_0/T clearly mimics the behavior of Tl-2201. This rapid increase of κ_0/T in magnetic field further rules out the case that the significant κ_0/T results from a small nonsuperconducting

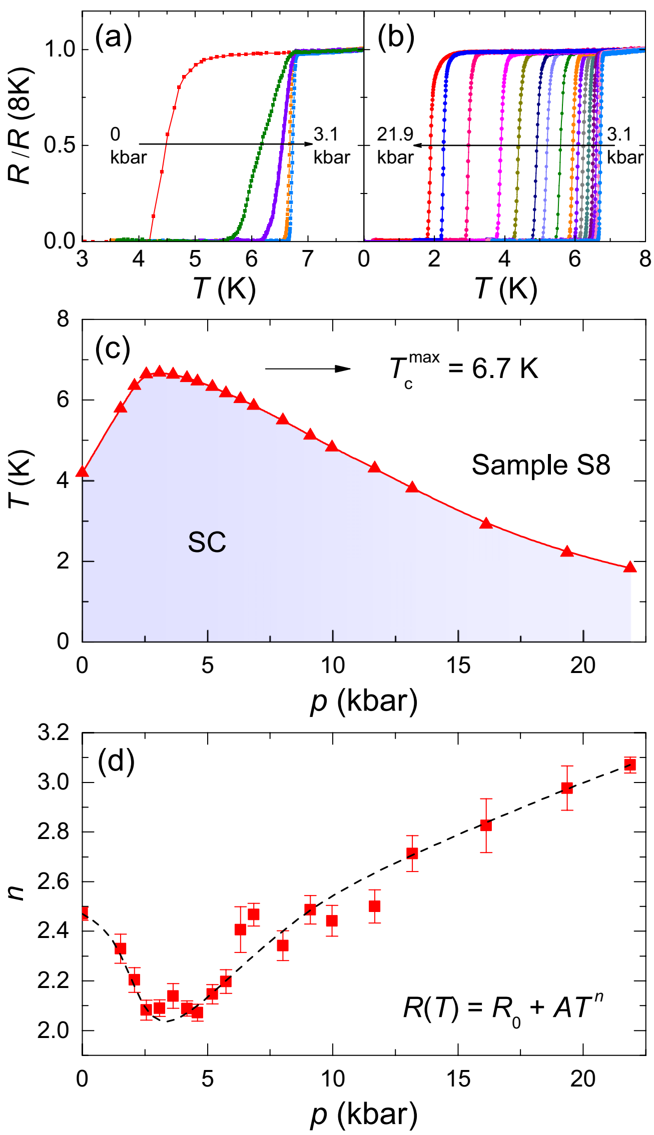

FIG. 5. (Color online) (a), (b) Low-temperature resistance of the $Ta_4Pd_3Te_{16}$ single crystal (sample S8) under various pressures up to 21.9 kbar. (c) The pressure-dependent T_c, defined by $\rho = 0$. There is a clear superconducting dome, with a maximum $T_c = 6.7$ K at optimal pressure $p_c = 3.1$ kbar. (d) The pressure dependence of the exponent n of resistance. There is a clear minimum of n near p_c.

metallic portion in the sample, since it should not change so dramatically in magnetic field. The rapid increase of κ_0/T in magnetic field should come from the Volovik effect of nodal quasiparticles, thus providing further evidence for nodes in the superconducting gap [16]. To our knowledge, so far all nodal superconductors have an unconventional pairing mechanism [1]. In this regard, the nodal gap we demonstrate from thermal conductivity results suggests unconventional superconductivity in $Ta_4Pd_3Te_{16}$.

To obtain further clues about the pairing mechanism in $Ta_4Pd_3Te_{16}$, we map out its temperature-pressure phase diagram by resistivity measurements under pressures. Figures 5(a) and 5(b) present the low-temperature resistivity of the $Ta_4Pd_3Te_{16}$ single crystal (sample S8) under various pressures up to 21.9 kbar. At ambient pressure, the T_c is 4.2 K, defined by $\rho = 0$. With increasing pressure, the T_c first increases sharply to 6.7 K at 3.1 kbar, enhanced by 60%. Then it decreases slowly to 1.8 K at 21.9 kbar. The nonmonotonic pressure dependence of T_c is plotted in Fig. 5(c), which shows a clear superconducting dome.

A temperature-pressure (T_c vs p) or temperature-doping (T_c vs x) superconducting dome has been commonly observed in many unconventional superconductors, including heavy-fermion superconductors, cuprate superconductors, iron-based superconductors, and Q2D organic superconductors [1]. For example, the heavy-fermion superconductor $CeCoIn_5$ manifests a T_c vs p superconducting dome, and the unconventional superconductivity with $d_{x^2+y^2}$ symmetry may result from the antiferromagnetic spin fluctuations [26]. Theoretically, it has been shown that unconventional superconductivity with d_{xy} symmetry can also appear in close proximity to a charge-ordered phase, and the superconductivity is mediated by charge fluctuations [27,28]. This may be the case of the pressure-induced superconductivity in $1T$-$TiSe_2$, with the superconducting dome appearing around the critical pressure related to the charge-density wave (CDW) meltdown [29].

For $Ta_4Pd_3Te_{16}$, recent electronic structure calculations showed that its electronic states are mostly derived from Te p states with small Ta d and Pd d contributions, which places the compound far from magnetic instabilities [13]. Two scanning tunneling microscopy (STM) studies on $Ta_4Pd_3Te_{16}$ found commensurate modulations along the atom chains, which may arise from CDW [30,31]. Recent Raman scattering experiments also revealed a possible CDW transition or the emergence of CDW fluctuations below a temperature in the 140–200 K range [32]. CDW usually appears in low-dimensional compounds, such as tetrathiafulvalene-tetracyanoquinodimethane (TTF-TCNQ), $NbSe_3$, and $NbSe_2$ [33–35], and therefore it is not surprising that CDW exists in layered $Ta_4Pd_3Te_{16}$ with a Q1D structure. The absence of a resistivity anomaly in the resistivity curve suggests that the CDW in $Ta_4Pd_3Te_{16}$ is quite weak, since the robustness of the CDW can be reflected from the resistivity anomaly, as seen in TTF-TCNQ, $NbSe_3$, and $NbSe_2$ [33–35].

To examine whether the superconducting dome relates to a CDW meltdown in $Ta_4Pd_3Te_{16}$, we carefully fit the resistance data up to 25 K to $\rho(T) = \rho_0 + AT^n$ for each pressure, and plot the pressure dependence of the exponent n in Fig. 5(d). There is a clear minimum of n near the optimal pressure $p_c = 3.1$ kbar. A similar pressure dependence of n has been observed in $1T$-$TiSe_2$ [29]. For $1T$-$TiSe_2$, the $n = 3$ at pressure above 40 kbar is attributed to the phonon-assisted s-d interband scattering, and the suppression of n in the 20–40 kbar pressure region signifies the presence of CDW fluctuations around a critical pressure of 30 kbar [29]. In this context, $p_c = 3.1$ kbar is likely the critical pressure where the CDW in $Ta_4Pd_3Te_{16}$ is completely suppressed. If this is the case, the nodal superconductivity in $Ta_4Pd_3Te_{16}$ may originate from the CDW fluctuations [27,28].

In summary, we study the superconducting gap structure of the layered superconductor $Ta_4Pd_3Te_{16}$ by low-temperature thermal conductivity measurements. The significant κ_0/T in zero magnetic field and its rapid field dependence suggest nodes in the superconducting gap. Further measurements of resistivity under pressure reveal a superconducting dome in the temperature-pressure phase diagram. These results indicate unconventional superconductivity in $Ta_4Pd_3Te_{16}$. With the recent STM and Raman evidence for the existence of CDW and our observation of the suppression of the exponent n near the optimal pressure p_c, $Ta_4Pd_3Te_{16}$ may provide a rare platform to study the unconventional superconductivity near a CDW instability. Clarifying the pairing symmetry and mechanism of this layered superconductor will give us understandings of unconventional superconductivity.

We thank X. H. Chen, J. K. Dong, and D. L. Feng for helpful discussions. This work is supported by the Natural Science Foundation of China, the Ministry of Science and Technology of China (National Basic Research Program No. 2012CB821402 and No. 2015CB921401), Program for Professor of Special Appointment (Eastern Scholar) at Shanghai Institutions of Higher Learning, STCSM of China (No. 15XD1500200), and Zhejiang Provincial Natural Science Foundation of China (No. LQ15A040005).

[1] M. R. Norman, The challenge of unconventional superconductivity, Science **332**, 196 (2011).
[2] C. C. Tsuei and J. R. Kirtley, Pairing symmetry in cuprate superconductors, Rev. Mod. Phys. **72**, 969 (2000).
[3] K. An, T. Sakakibara, R. Settai, Y. Onuki, M. Hiragi, M. Ichioka, and K. Machida, Sign Reversal of Field-Angle Resolved Heat Capacity Oscillations in a Heavy Fermion Superconductor $CeCoIn_5$ and $d_{x^2-y^2}$ Pairing Symmetry, Phys. Rev. Lett. **104**, 037002 (2010).
[4] A. P. MacKenzie and Y. Maeno, The superconductivity of Sr_2RuO_4 and the physics of spin-triplet pairing, Rev. Mod. Phys. **75**, 657 (2003).
[5] P. J. Hirschfeld, M. M. Korshunov, and I. I. Mazin, Gap symmetry and structure of Fe-based superconductors, Rep. Prog. Phys. **74**, 124508 (2011).
[6] D. Jérome, A. Mazaud, M. Ribault, and K. Beechgard, Superconductivity in a synthetic organic conductor $(TMTSF)_2PF_6$, J. Phys. Lett. **41**, 95 (1980).
[7] K. Bechgaard, K. Carneiro, M. Olsen, F. B. Rasmussen, and C. S. Jacobsen, Zero-Pressure Organic Superconductor: Di-(tetramethyltetraselenafulvalenium)-Perchlorate $[(TMTSF)_2ClO_4]$, Phys. Rev. Lett. **46**, 852 (1981).
[8] W. Zhang and C. A. R. Sá de Melo, Triplet versus singlet superconductivity in quasi-one-dimensional conductors, Adv. Phys. **56**, 545 (2007).
[9] I. I. Mazin, Perspective article superconductivity gets an iron boost, Nature (London) **464**, 183 (2010).
[10] A. Mar and J. A. Ibers, Synthesis, crystal structure and electrical conductivity of a new layered ternary telluride $Ta_4Pd_3Te_{16}$, J. Chem. Soc., Dalton Trans., 639 (1991).
[11] W. H. Jiao, Z. T. Tang, Y. L. Sun, Y. Liu, Q. Tao, C. M. Feng, Y. W. Zeng, Z. A. Xu, and G. H. Cao, Superconductivity in a layered $Ta_4Pd_3Te_{16}$ with $PdTe_2$ chains, J. Am. Chem. Soc. **136**, 1284 (2014).
[12] J.-F. Mercure, A. F. Bangura, X. F. Xu, N. Wakeham, A. Carrington, P. Walmsley, M. Greenblatt, and N. E. Hussey, Upper Critical Magnetic Field far above the Paramagnetic Pair-Breaking Limit of Superconducting One-Dimensional $Li_{0.9}Mo_6O_{17}$ Single Crystals, Phys. Rev. Lett. **108**, 187003 (2012).
[13] D. J. Singh, Multiband superconductivity of $Ta_4Pd_3Te_{16}$ from Te p states, Phys. Rev. B **90**, 144501 (2014).
[14] I. J. Lee, M. J. Naughton, G. M. Danner, and P. M. Chaikin, Anisotropy of the Upper Critical Field in $(TMTSF)_2PF_6$, Phys. Rev. Lett. **78**, 3555 (1997).
[15] G. Mihály, I. Kézsmárki, F. Zámborszky, and L. Forró, Hall Effect and Conduction Anisotropy in the Organic Conductor $(TMTSF)_2PF_6$, Phys. Rev. Lett. **84**, 2670 (2000).
[16] H. Shakeripour, C. Petrovic, and L. Taillefer, Heat transport as a probe of superconducting gap structure, New J. Phys. **11**, 055065 (2009).
[17] M. Sutherland, D. G. Hawthorn, R. W. Hill, F. Ronning, S. Wakimoto, H. Zhang, C. Proust, Etienne Boaknin, C. Lupien, L. Taillefer, R. X. Liang, D. A. Bonn, W. N. Hardy, R. Gagnon, N. E. Hussey, T. Kimura, M. Nohara, and H. Takagi, Thermal conductivity across the phase diagram of cuprates: Low-energy quasiparticles and doping dependence of the superconducting gap, Phys. Rev. B **67**, 174520 (2003).
[18] S. Y. Li, J.-B. Bonnemaison, A. Payeur, P. Fournier, C. H. Wang, X. H. Chen, and L. Taillefer, Low-temperature phonon thermal conductivity of single-crystalline Nd_2CuO_4: Effects of sample size and surface roughness, Phys. Rev. B **77**, 134501 (2008).
[19] S. Y. Li, L. Taillefer, G. Wu, and X. H. Chen, Single-Gap s-Wave Superconductivity near the Charge-Density-Wave Quantum Critical Point in Cu_xTiSe_2, Phys. Rev. Lett. **99**, 107001 (2007).
[20] J. K. Dong, S. Y. Zhou, T. Y. Guan, H. Zhang, Y. F. Dai, X. Qiu, X. F. Wang, Y. He, X. H. Chen, and S. Y. Li, Quantum Criticality and Nodal Superconductivity in the FeAs-Based Superconductor KFe_2As_2, Phys. Rev. Lett. **104**, 087005 (2010).
[21] C. Proust, E. Boaknin, R. W. Hill, L. Taillefer, and A. P. Mackenzie, Heat Transport in a Strongly Overdoped Cuprate: Fermi Liquid and a Pure d-Wave BCS Superconductor, Phys. Rev. Lett. **89**, 147003 (2002).
[22] M. Suzuki, M. A. Tanatar, N. Kikugawa, Z. Q. Mao, Y. Maeno, and T. Ishiguro, Universal Heat Transport in Sr_2RuO_4, Phys. Rev. Lett. **88**, 227004 (2002).
[23] J. Lowell and J. B. Sousa, Mixed-state thermal conductivity of type II superconductors, J. Low. Temp. Phys. **3**, 65 (1970).
[24] J. Willis and D. Ginsberg, Thermal conductivity of superconducting alloy films in a perpendicular magnetic field, Phys. Rev. B **14**, 1916 (1976).
[25] E. Boaknin, M. A. Tanatar, J. Paglione, D. Hawthorn, F. Ronning, R. W. Hill, M. Sutherland, L. Taillefer, J. Sonier, S. M. Hayden, and J. W. Brill, Heat Conduction in the Vortex State of $NbSe_2$: Evidence for Multiband Superconductivity, Phys. Rev. Lett. **90**, 117003 (2003).
[26] V. A. Sidorov, M. Nicklas, P. G. Pagliuso, J. L. Sarrao, Y. Bang, A. V. Balatsky, and J. D. Thompson, Superconductivity and Quantum Criticality in $CeCoIn_5$, Phys. Rev. Lett. **89**, 157004 (2002).
[27] D. J. Scalapino, E. Loh, and J. E. Hirsch, Fermi-surface instabilities and superconducting d-wave pairing, Phys. Rev. B **35**, 6694 (1987).

[28] J. Merino and R. H. McKenzie, Superconductivity Mediated by Charge Fluctuations in Layered Molecular Crystals, Phys. Rev. Lett. **87**, 237002 (2001).

[29] A. F. Kusmartseva, B. Sipos, H. Berger, L. Forró, and E. Tutiš, Pressure Induced Superconductivity in Pristine $1T$–$TiSe_2$, Phys. Rev. Lett. **103**, 236401 (2009).

[30] Z. Du, D. Fang, Z. Wang, Y. Li, G. Du, H. Yang, X. Zhu, and H.-H. Wen, Anisotropic superconducting gap and elongated vortices with Caroli-De Gennes-Matricon states in the new superconductor $Ta_4Pd_3Te_{16}$, Sci. Rep. **5**, 9408 (2015).

[31] Q. Fan, W. H. Zhang, X. Liu, Y. J. Yan, M. Q. Ren, M. Xia, H. Y. Chen, D. F. Xu, Z. R. Ye, W. H. Jiao, G. H. Cao, B. P. Xie, T. Zhang, and D. L. Feng, Scanning tunneling microscopy study of superconductivity, magnetic vortices, and possible charge-density wave in $Ta_4Pd_3Te_{16}$, Phys. Rev. B **91**, 104506 (2015).

[32] D. Chen, P. Richard, Z.-D. Song, W.-L. Zhang, S.-F. Wu, W. H. Jiao, Z. Fang, G.-H. Cao, and H. Ding, Raman scattering investigation of quasi-one-dimensional superconductor $Ta_4Pd_3Te_{16}$, arXiv:1505.05247.

[33] A. Andrieux, H. J. Schulz, D. Jerome, and K. Bechgaard, Conductivity of the One-Dimensional Conductor Tetrathiafulvalene-Tetracyanoquinodimethane (TTF-TCNQ) near Commensurability, Phys. Rev. Lett. **43**, 227 (1979).

[34] A. Briggs, P. Monceau, M. Nunez-Regueiro, J. Peyrard, M. Ribaultl, and J. Richard, Charge density wave formation, superconductivity and Fermi surface determination in $NbSe_3$: a pressure study, J. Phys. C: Solid State Phys. **13**, 2117 (1980).

[35] H. N. S. Lee, H. McKinzie, D. S. Tannhauser, and A. Wold, The low-temperature transport properties of $NbSe_2$, J. Appl. Phys. **40**, 602 (1969).